

Upcycling Waste Biomass–Production of Porous Carbonaceous Supports from Paper Mill Sludge and Application to CO₂ Conversion

Mónica Stanton Ribeiro, Maria M. R. A. Lima, Márcia Vilarigues, Marcileia Zanatta,* and Marta C. Corvo*

The urgent need for sustainable waste management strategies has led to the exploration of innovative approaches for the valorization of waste. In this study, a method is proposed for carbonizing waste biomass materials, particularly paper mill waste sludges (primary and biological) and knots, to produce porous carbonaceous supports. Through an initial hydrothermal carbonization followed by carbonization with nitrogen flow, porous carbon materials are successfully generated. The findings of this investigation validate the successful generation of effective carbonaceous supports utilizing waste biomass materials. These materials are then evaluated for their effectiveness as porous supports in the ionic liquid-catalyzed cycloaddition reaction of CO₂ to styrene oxide, achieving a remarkable conversion rate of up to 98% and an impressive selectivity exceeding 99%. Additionally, the results underscore the significant impact of the selected IL on the overall conversion process. Overall, this study presents a promising pathway for the valorization of paper mill waste sludge through the production of porous carbon materials with potential applications in catalysis and beyond.

1. Introduction

The adoption of circular economy approaches emerges as a pivotal strategy for substantial reductions in greenhouse gas emissions. The reuse of solid and gas wastes are two paths toward sustainable resource management, and in this context, upcycling waste can extend the usefulness of materials and reduce their environmental impact. Regarding solid waste, biomass materials are an increasingly popular source of recyclable waste because they offer not only a wide availability and renewability but also the flexibility to adjust their physical and chemical characteristics, rendering them highly attractive for several applications, including as heterogeneous catalysts and support for carbon dioxide (CO₂) conversion.^[1–5] As for the gaseous waste

materials, the alarming rise in CO₂ emissions has also prompted the global community for sustainable development and circular economy solutions. The conversion of CO₂ into added-value products can respond to this need. The combined characteristics of being a low-cost and non-toxic by-product of fossil fuel combustion and its abundance in nature, make the use of CO₂ very appealing to the scientific community.^[6] In this field, the transformation of this gas into added-value products is a topic that has gathered great interest due to the call for greener chemistry.

Conversion products such as methanol,^[7] dimethyl carbonate,^[8] urea,^[9] carboxylic acids,^[10] or, most commonly, cyclic carbonates^[11] can be used in a wide variety of applications, from plastics and resin materials to solvents for battery electrolytes and important chemical intermediates in the pharmaceutical industry.^[12]

Independently of the products desired from CO₂ conversion, it involves a reaction that cannot be performed on its own due to the elevated thermodynamic stability of this gas. To decrease the activation energy of the desired reaction, highly energetic starting materials (hydrogen, epoxides, amines, etc.) and catalysts are used in conjunction to curb the fact that the carbon atom in the CO₂ molecule is in its most oxidized state, and, consequently, shows low molecular reactivity.^[13] Catalysts can be classified as heterogeneous when they are in a different phase than the reactants, or as homogeneous when they are in

M. S. Ribeiro, M. M. R. A. Lima, M. C. Corvo
i3N|Cenimat

Materials Science Department
NOVA School of Science and Technology
NOVA University Lisbon
Caparica 2829-516, Portugal
E-mail: marta.corvo@fct.unl.pt

M. Vilarigues
Vicarte

Conservation and Restoration Department
NOVA School of Science and Technology
NOVA University Lisbon
Caparica 2829-516, Portugal

M. Zanatta
Institute of Advanced Materials (INAM)
Universitat Jaume I
Castellón 12071, Spain
E-mail: zanatta@uji.es

 The ORCID identification number(s) for the author(s) of this article can be found under <https://doi.org/10.1002/adsu.202300655>

© 2024 The Authors. Advanced Sustainable Systems published by Wiley-VCH GmbH. This is an open access article under the terms of the [Creative Commons Attribution](#) License, which permits use, distribution and reproduction in any medium, provided the original work is properly cited.

DOI: 10.1002/adsu.202300655

the same phase as the reactants.^[14] Typical homogeneous catalysts for CO₂ conversion are metal complexes,^[15] ionic liquids (ILs),^[16] superbases,^[17] and organocatalysts.^[18] Typical heterogeneous catalysts include poly(ionic liquid)s (PILs),^[19,20] metal-organic frameworks,^[21] porous carbons,^[22] silica sieves,^[23] and metal oxides.^[24]

One expeditious approach to catalysis consists of heterogenizing a homogeneous catalyst by supporting it on a porous material, producing a *hybrid catalyst*. This method gathers the advantages of both homogeneous and heterogeneous catalysts, with improved stability, recyclability, control, and versatility in catalytic processes. One of the main features concerns the possibility of achieving a high dispersion of the catalyst active sites by modulating the relation between surface area and porosity to the total catalyst loading.^[25,26] Several supports, including polymer resins, silica nanomaterials, metal-organic frameworks (MOFs), and carbon materials, have been developed to convert homogeneous catalysts into industrially favored heterogeneous catalysts.^[27] Amongst these examples, porous carbon materials may be one of the most promising due to their many unique properties, which include low cost, potential for increased active sites through heteroatom doping, high surface area, and high porosity.^[28] These carbon materials can even be prepared from inexpensive, highly renewable, and eco-friendly materials, such as biomass.^[29–32] Examples of biomass that have been studied in the field of carbon capture and storage range from commercially available materials such as chitosan,^[33,34] glucose,^[35] algae,^[29] and cellulose,^[36] to materials derived from other industries, such as waste cow manure,^[28] rice husk,^[1,37–40] wood sawdust,^[41] cocoa bean shells,^[42] or waste sludges.^[43–47] The natural abundance of functional groups in biomass materials, like hydroxyl, carboxyl, or aldehyde groups, is one of the properties that has been found to play an important role in the cycloaddition reaction of CO₂ to epoxides.^[48]

Although it is more common to rely on carbonization-activation methods to produce porous carbons from biomass materials, additives can also be incorporated into the system as carbon precursors to induce further porosity, such as ILs. ILs are organic salts that exist freely and stably in liquid form at temperatures below 100 °C. Usually, they are composed of a large nitrogen or phosphorous-containing cation (e.g., imidazolium or phosphonium, respectively), where the anion is much smaller and can be organic (e.g., bis(trifluoromethylsulfonyl)imide (NTf₂⁻) or dicyanamide (N(CN)₂⁻)) or inorganic (e.g., Cl⁻ or tetrafluoroborate (BF₄⁻)).^[49]

Despite being identified over a century ago, back in 1914,^[50] ILs remain a subject of ongoing interest for scientists due to their exceptional physical and chemical attributes. These include their low vapor pressure, robust thermal, photochemical, electrochemical, and chemical stability, as well as their non-flammable nature. Additionally, the ability to combine various anions and cations in different configurations enables the creation of a plethora of compounds, each possessing unique properties that influence their solubility and selectivity toward CO₂.^[51–53] As such, ILs have been used as templates in soft-templating carbonization,^[54] solvents in ionothermal carbonization,^[55] and in other variations of these techniques, such as self-templating,^[56] salt-templating,^[57,58] and confined carbonization.^[59] The benefits of using ILs and biomass for car-

bon precursors rely on attaining high N/C ratios and average pore diameters. Furthermore, the combined utilization of both materials as carbon precursors results in the production of carbons exhibiting remarkable surface areas and total pore volumes.^[60]

To explore an environmentally sustainable approach for the synthesis of catalyst supports, this study investigates the potential of carbon-based materials derived from the carbonization of biomass, including chitosan and knots and waste sludges from a paper mill operation. Furthermore, the aim is to assess the role that ILs and other additives have in the carbonization yield, nitrogen content, porosity, and conversion for the cycloaddition reaction of CO₂ to styrene oxide (SO). Most studies in this field do not use ILs as carbon precursors but rather immobilize them onto the surface of the biomass-based carbon.^[28,38] The use of both biomass and ILs as carbon precursors is, however, applied in other areas such as supercapacitors,^[61] and CO₂ capture.^[34] Herein, we propose applying metal-free carbon materials prepared with different types of biomass (chitosan, paper mill waste sludges, and knots) and IL precursors (**Figure 1A,B**) in the development of porous materials to enable the IL-supported solvent-free CO₂ conversion. Chitosan is a commercial product derived from chitin from shellfish processing. Paper mills generate biomass that provides precursors for biomaterials such as lignin, hemicellulose, cellulose, and nanocellulose.^[62,63] Paper mill waste materials have already been upcycled as feedstock for renewable fuels and chemicals production.^[64,65] Here, we study the utilization of these two polysaccharide-derived waste materials for the production of porous carbons, and explore their use as supports for the IL catalyzed CO₂ conversion.

2. Experimental Section

2.1. Preparation of Porous Carbons

2.1.1. Pre-Carbonization Processes

1-Butyl-3-methylimidazolium chloride ([Im]Cl) was dried under vacuum for 2 h before use. 1-Butyl-4-methylpyridinium chloride ([4py]Cl) was dried under vacuum overnight at 50 °C before use. Paper mill waste sludges (primary and biological) and knots were dried under vacuum at 105 °C for 2 h. They were then ground and sieved to obtain uniform powders that were stored until used.

2.1.2. Carbonization

The present methodology was adapted from a previous report by Wu et al.^[66] In a typical experiment, 500 mg of selected biomass material, 250 mg of additive (IL or salt mixture), and 5 mL of water were stirred at 50 °C for 60 min to obtain a suspension. This suspension was then inserted into a 45 mL Parr reactor, placed into an oil bath, and heated to 180 °C for 17 h. The reactor was then placed in an ice bath to cool down. The resulting product was collected, centrifuged at 12 000 rpm for 5 min, washed with water until the solution was clear, and washed one final time with ethanol. The solid was then dried overnight at 100 °C. The resulting powder was placed in a tubular alumina furnace under nitrogen atmosphere. The furnace containing the sample was purged with nitrogen flowing at 75 mL min⁻¹ for 30 min at room temperature. The nitrogen flow was then reduced to 10–20 mL min⁻¹

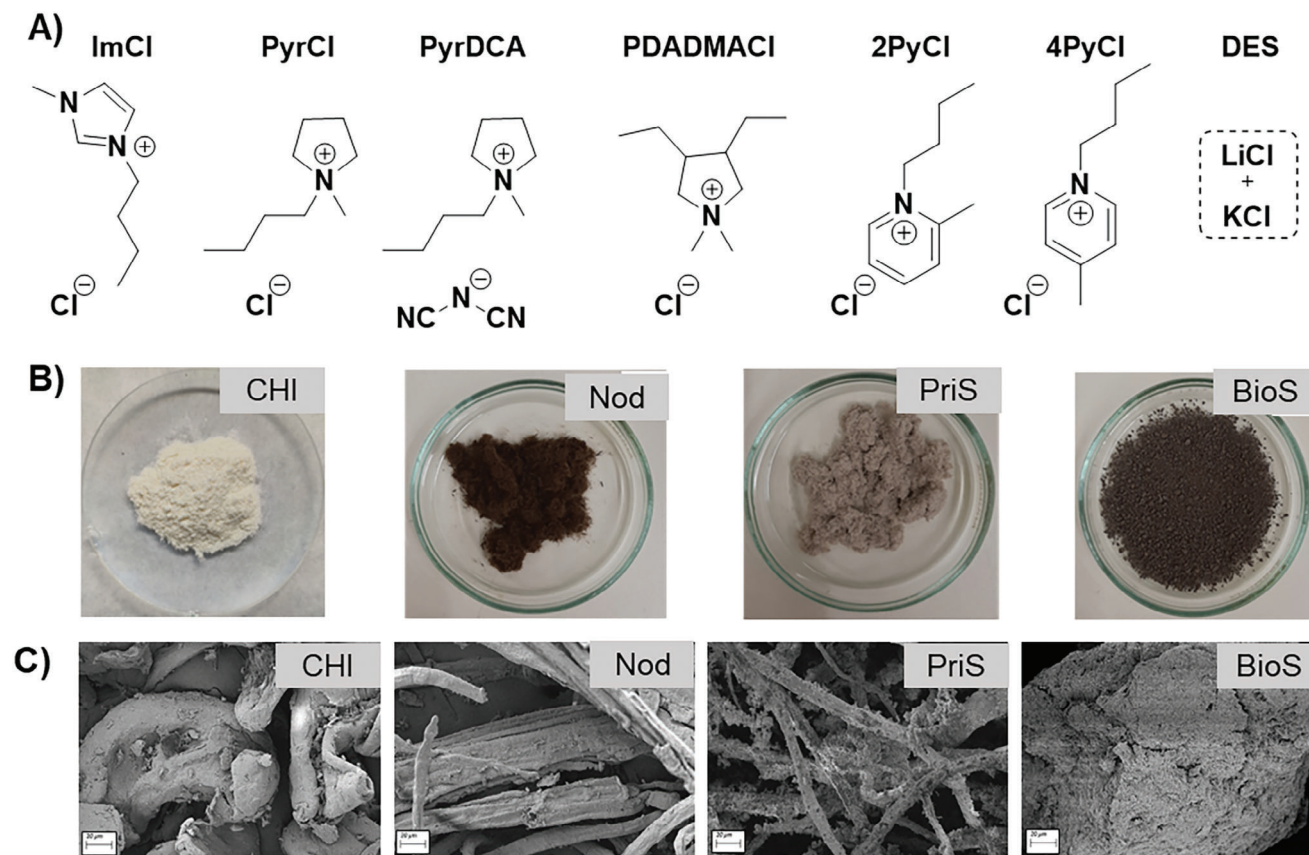


Figure 1. A) ILs and B) biomass used in this work. C) SEM images of starting material.

and the furnace was heated at a rate of $15\text{ }^{\circ}\text{C min}^{-1}$ to $800\text{ }^{\circ}\text{C}$ for 2 h. After the dwell was completed, the nitrogen flow was interrupted and, by switching off the power, the furnace cooled down to room temperature.

Carbonization of the biomass materials (Figure 1B) was also performed without additives, following all the steps described above. The complete carbonizations are listed in Table S1 (Supporting Information). The samples were then characterized through elemental analysis, nitrogen adsorption/desorption isotherms, Scanning Electron Microscopy (SEM), and Raman spectroscopy. The SEM images of starting materials can be seen in Figure 1C.

2.1.3. Post-Carbonization Processes

After carbonization, the sample prepared from chitosan (CHI) and the salt mixture LiCl/KCl (CHI-DES) was washed and filtered with sufficient water to remove any remaining salt. The sample was then dried at $40\text{ }^{\circ}\text{C}$ under vacuum for over 42 h and designated CHI-DES-F.

2.2. Cycloaddition of CO_2 and Recyclability

In a typical experiment, a certain amount of SO , porous carbon, and catalyst, tetrabutylammonium bromide (TBABr), tetrabutyl-

ammonium chloride (TBACL), vinylbenzyltriethylammonium chloride (VBACL) or poly(vinylbenzyltriethylammonium) chloride (PVBACL) were placed in a Parr reactor. The reactor was purged three times with cycles of vacuum and CO_2 , to evacuate the air from the inside of the equipment, and then charged to 5 bar of CO_2 . The reactor was placed in an oil bath previously heated to $100\text{ }^{\circ}\text{C}$ for a designated time. When the reaction time was complete, the reactor was placed into an ice bath to cool down.

After this, all the product from the reaction was transferred from the reactor to an Eppendorf tube, which was centrifuged, and the supernatant was separated from the porous carbon, into an NMR test tube. This supernatant was then analyzed by ^1H NMR to assess the outcome of the reaction (Figure S6, Supporting Information).

To assess the recyclability of the porous carbon, after completing all the steps described previously, the remaining carbon material was washed, shaken, and centrifuged with $500\text{ }\mu\text{L}$ of trichloromethane twice. Both times, the supernatant was removed after centrifuging, so to eliminate all traces of the catalyst. The washed product was then placed under vacuum for 22 h at $35\text{ }^{\circ}\text{C}$, after which the porous carbon was reused in a subsequent reaction under the same conditions, by adding SO , catalyst, and more porous carbon to compensate the amount lost in the washing. The conversion of the reactions was assessed using ^1H NMR after every cycle.

Table 1. Elemental analysis, carbonization yield, textural and structural parameters for the studied samples.

Entry	Sample name	Average Carbonization Yield [wt.%]	N ^{a)} [wt.%]	C ^{a)} [wt.%]	H ^{a)} [wt.%]	I _D /I _G ^{b)}	Average pore width [nm] ^{c)}
1	Knots	–	0.11	44.18	5.04	–	–
2	Primary Sludge	–	0.63	29.88	3.73	–	–
3	Biological Sludge	–	2.74	33.52	3.97	–	–
4	CHI	–	6.94	40.15	6.88	–	–
5	Kno-0	22	0.24	72.18	0.43	1.09	–
6	PriS-0	37	0.11	7.02	0.82	1.36	–
7	BioS-0	41	0.15	9.07	0.44	1.35	–
8	BioS-ImCl	38	0.31	9.42	1.78	1.22	–
9	CHI-0	32	7.14	47.49	0.71	1.14	–
10	CHI-ImCl	30	6.69	74.70	1.45	1.19	–
11	CHI-2PyCl	29	6.89	77.40	0.99	1.16	122
12	CHI-4PyCl	32	7.23	78.46	1.06	1.17	84
13	CHI-PyrCl	28	6.91	76.97	1.06	1.22	–
14	CHI-PyrDCA	27	8.04	76.32	1.12	1.05	88
15	CHI-PDADMACl	28	7.35	73.49	0.95	1.30	40–80
16	CHI-DES	40	5.02	53.11	1.06	1.09	–
17	CHI-DES-F	29	6.79	70.05	0.82	–	364

^{a)} Values obtained from elemental analysis; ^{b)} Values obtained from Raman spectroscopy (Figures S1–S3, Supporting Information); ^{c)} Values obtained directly from ImageJ.

3. Results and Discussion

3.1. Porous Carbon Characterization

Metal-free carbon samples were produced by a two-step procedure, namely a hydrothermal carbonization followed by a carbonization with nitrogen flow, as described in the experimental part. All samples were subsequently thoroughly analyzed. **Table 1** summarizes the elemental analysis, carbonization yield, and textural and structural parameters of the samples used and produced in this study.

The paper mill waste biomass originated the samples with both the highest and lowest carbonization yield. The lowest carbonization yield of 22 wt.% was obtained with the knots (Entry 5 of **Table 1**) while the highest carbonization yields were obtained with the samples prepared from the biological sludge (Entries 7 and 8 of **Table 1**). This is a good indicator of the feasibility of using waste sludges from the paper and pulp industry as a carbon precursor. Regarding the carbons prepared with chitosan, the carbonization yield of these falls in the range of 27 to 32 wt.%, except for sample CHI-DES (carbonization yield of 40 wt.%) but after washing, the carbonization yield lowered to 29 wt.% (Entries 16 and 17 of **Table 1**, respectively). The lowest carbonization yield obtained with chitosan was for the samples whose additive was a pyrrolidinium-based IL (Entries 13 to 15 of **Table 1**), which is in agreement with the literature.^[67] Overall, the incorporation of additives, whether IL or salt mixture, did not increase the carbonization yield, both in the case of the samples prepared from waste biomass and chitosan.

Generally, the carbonization process caused an increase in carbon content and a decrease in nitrogen and hydrogen content (**Table 1**), which is expected, since this process enriches the ma-

trix in carbon and removes heterogenous elements, what is left behind is a skeleton with an improved carbon content and a reduced nitrogen and hydrogen content.^[68] Elemental analysis of the carbon samples shows that the average nitrogen content increases in the following order of IL cation type: imidazolium < pyridinium < pyrrolidinium. Sun et al. reported similar results to those obtained in the present study.^[69] As mentioned previously, carbonization tends to increase the carbon content of the material, however, for sludges, the opposite is more common,^[43] which is the case with both paper mill sludges analyzed, primary and biological.

Raman spectra of these samples (**Figure 2A**) show that the characteristic D ($\approx 1327\text{ cm}^{-1}$ in green) and G bands ($\approx 1582\text{ cm}^{-1}$ in blue) are present in all the carbon samples.^[70] These bands are related to the defective/disordered structure of the carbon and the in-plate vibration of the sp^2 carbon atoms, respectively. The ratio of their intensities (I_D/I_G in **Table 1**) is used to evaluate the degree of graphitization of the carbon, such that a higher intensity ratio points to a more disordered structure and thus, a lower degree of graphitization.^[22,34,71,72] Overall, all samples show relatively high-intensity ratios. Sample CHI-PDADMACl that presents low degrees of graphitization (Entry 15 of **Table 1**) has the highest intensity ratio among those prepared with chitosan, which could be related to the fact that the additive PDADMACl used as a precursor was a 20 wt.% solution in H_2O , resulting in excess water present during the hydrothermal carbonization compared to the other samples. Samples prepared with the biological sludge present a single peak at around 1080 cm^{-1} , observable in **Figure 2A**, which indicates the presence of carbonate ions.^[73] This presence, also encountered by Jaria et al.,^[74] can be justified by the use of calcium carbonate as a blanching agent for pulp and paper production. The presence of this material

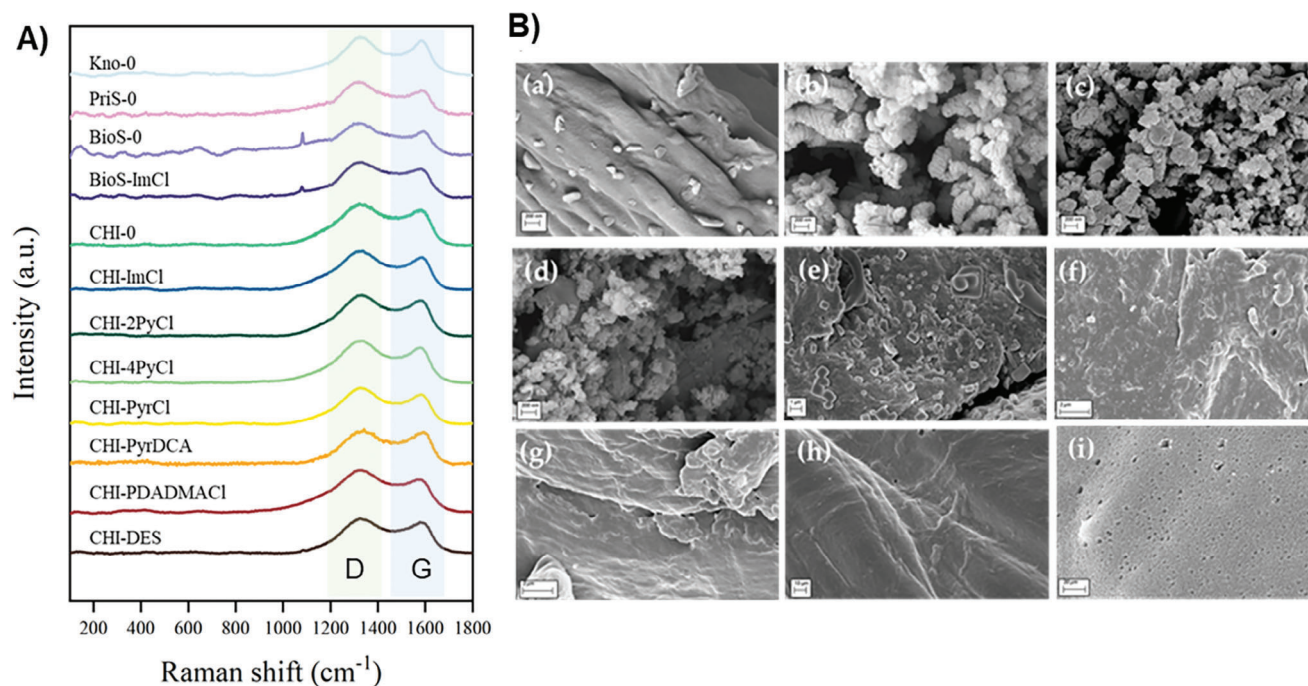


Figure 2. A) Raman spectra of the porous carbons produced. B) SEM images of samples a) Kno-0; b) PriS-0; c) BioS-0; d) BioS-ImCl; e) CHI-DES; f) CHI-2PyCl; g) CHI-4PyCl; h) CHI-PyrDCA; i) CHI-PDADMACl.

in the paper mill sludges is corroborated also by the detection of an elevated amount of calcium in SEM-EDS (Figures S4 and S5, Supporting Information). Furthermore, although chitosan-derived samples are mainly composed of carbon and nitrogen, the biological sludges show a variety of elements besides carbon and calcium, including silicon, magnesium, and phosphorus.

Most of the obtained carbons showed no porosity or macroporosity through the analysis of the N_2 adsorption/desorption isotherms, according to the International Union of Pure and Applied Chemistry (IUPAC),^[75] which also categorizes the type of porosity based on the pore size of the material: microporosity (<2 nm), mesoporosity (2–50 nm), or macroporosity (>50 nm). SEM images of samples CHI-PyrDCA, CHI-PDADMACl, CHI-2PyCl, CHI-4PyCl, and CHI-DES-F (Figure 2B), analyzed with the software *ImageJ*, corroborate that these samples possess macroporosity and some mesoporosity (in the case of sample CHI-PDADMACl), as shown in Table 1. Samples CHI-0 and CHI-PyrCl showed a Type I/II isotherm, which indicated that they both possessed micro/macroporosity (Figure S3b, Supporting Information). By cross-referencing the information from the N_2 adsorption/desorption isotherms and the pore width values obtained with *ImageJ*, the pore sizes of the chitosan-based carbonized samples are shown to increase in the following order of cation type: pyrrolidinium < pyridinium < imidazolium, where the PIL with a pyrrolidinium base (sample CHI-PDADMACl) produced larger pores than its IL counterpart (sample CHI-PyrCl). A similar result can be found in the literature and is believed to be a result of the multivalent binding power of the PIL.^[76] The paper mill sludges, both primary and biological, have a Type III isotherm and the knots have a Type II, which indicates that these samples are macroporous or non-porous, which is confirmed with SEM images (Figure 2B; Figure S3, Supporting Infor-

mation). The absence of mesoporosity on the paper mill sludges can be a consequence of the more heterogeneous elemental nature of these samples.

3.2. Catalysis Performance

To properly analyze the conversions obtained, it is essential to have a comprehensive understanding of the conversion mechanism of the cycloaddition of CO_2 to epoxides (Figure 3A) and potential influences. The conversion process entails three primary stages: initially, activation of the epoxide occurs, leading to the opening of the oxirane ring by a nucleophilic group; subsequently, the CO_2 molecule inserts into the resulting oxygen anion intermediate, followed by the closure of the ring to generate the cyclic carbonate. Finally, the nucleophilic group is regenerated for subsequent reactions.^[77]

The crucial step in determining the reaction rate involves the nucleophilic opening of the epoxide ring.^[78] The epoxide is usually activated by a Lewis acid, either a transition metal or a HBD. Typically, the epoxide is activated by a Lewis acid, such as a transition metal or a HBD, which binds to the oxygen atom of the epoxide through hydrogen bonding, thereby activating it. Subsequently, the ring can be opened through nucleophilic attack at the less sterically hindered carbon of the epoxide.^[79] Consequently, an effective catalytic system for this reaction would typically involve a combination of a Lewis acid center with highly nucleophilic groups.^[80] Biomass materials generally possess a limited number of reactive sites, most of which are HBD groups, such as hydroxyl, methoxy, aldehyde, ketone, and carboxyl, among others. Lewis bases can also help speed up the conversion mechanism

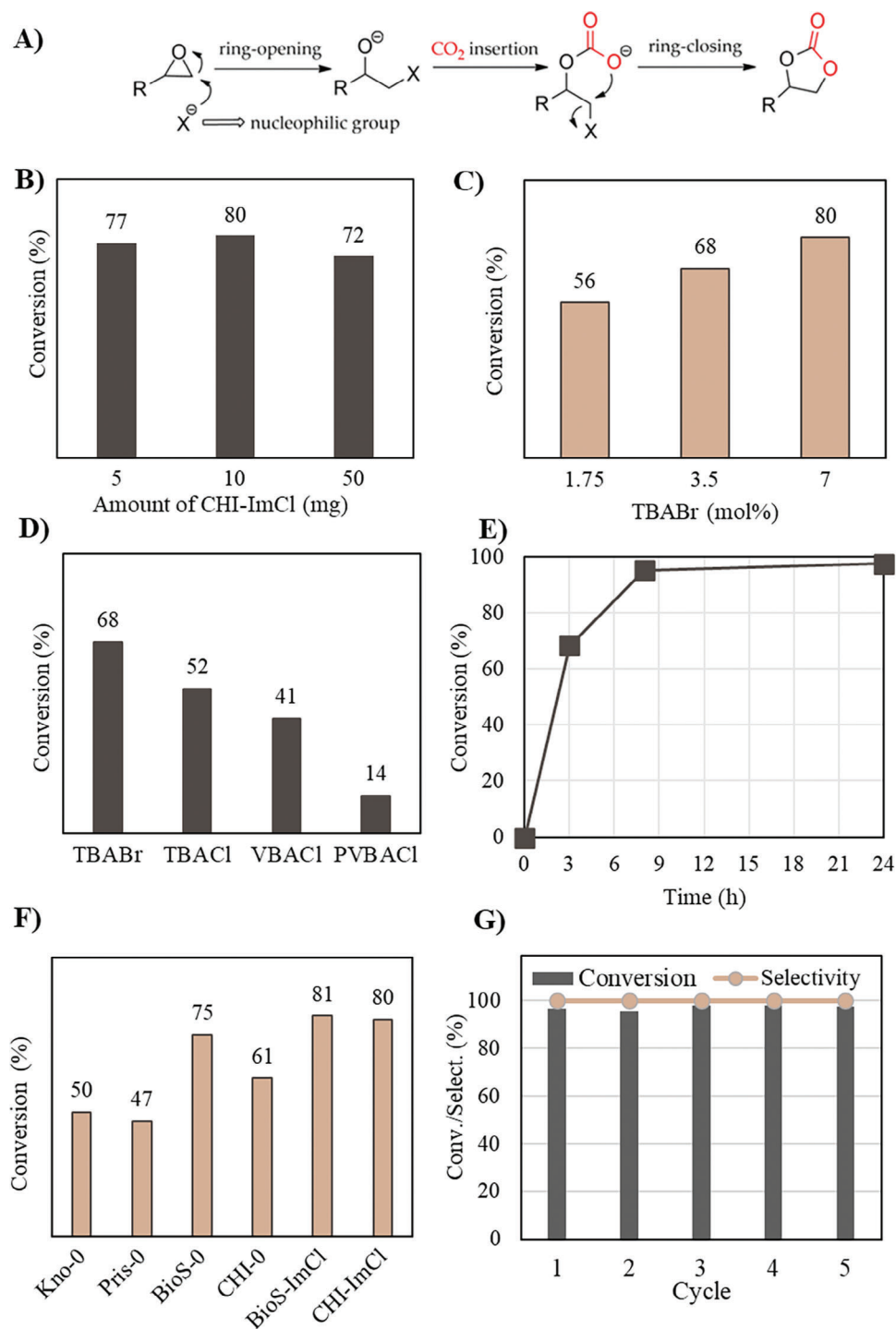


Figure 3. A) Generally accepted mechanism of the cycloaddition reaction of epoxides with CO₂. Catalytic activity experiments: B) Influence of the amount of CHI-ImCl; C) Influence of the molar percentage of catalyst TBABr concerning SO; D) Influence of type catalyst; E) Influence of time; F) Influence of porous carbon; G) Recycle tests (24 h of reaction); *General reaction conditions:* 100 °C, 3 h, CO₂ (5 bar), SO (6.67 mmol), TBABr (3.5 mol%), CHI-ImCl (10 mg).

by activating the CO₂, as occurs with the addition of ILs and deep eutectic salt mixtures.^[48]

The porous carbons synthesized in this study were impregnated with ammonium derived ILs as catalysts, producing the hybrid catalysts that were tested in the cycloaddition of CO₂ to styrene epoxide. The reaction was screened for the optimal conditions using CHI-ImCl, the amount and type of catalyst, the reaction duration, and finally, the nature of the porous carbon (Figure 3). The amount of CHI-ImCl was changed between 5 and 50 mg, which amounts to a variation between 0.6 and 6.2 wt.% toward SO. It is possible to observe that the conversion in cyclic carbonate increases with the amount of CHI-ImCl up the 1.25 wt.% attaining 80% yield and decreases for further increment (Figure 3B), an expected trend due to the active sites.^[2] The conversion reaction also reaches a saturation point, thus the increase of the amount of porous carbons to 50 mg did not favor an increment of the conversion. This phenomenon agrees with the study carried out by Sun et al.^[81] where catalyst loading above 1.8 mol% resulted in a lowered conversion for the cycloaddition of CO₂ to propylene oxide. The decreased conversion for a higher amount of porous carbon was attributed to an ineffective dispersion of the catalyst in the reaction mixture that limited the mass transfer between the active sites and the reactants. All the reactions exhibited a selectivity >99%, no other reaction product was detected.

The molar percentage of catalyst TBABr was altered in the presence and absence of the porous carbon CHI-ImCl, maintaining all other parameters constant (Figure 3C). This parameter was tested to determine the conditions for improved conversion using the CHI-ImCl. The decrease in the amount of catalyst caused a decrease in the conversion, which is expected. The bromide anion of the co-catalyst has strong nucleophilicity,^[38] which means that it facilitates the ring-opening process and effectively acts as a leaving group, so to be easily displaced and ensure the formation of the cyclic carbonate.^[82] As such, the increase in the amount of catalyst being accompanied by an improvement in conversion is due to the presence of additional nucleophiles.^[15] Using 3.5 mol% of TBABr catalyst was observed to produce a more noticeable improvement in the conversion, being lower than the co-catalyst molar percentages used in the literature.^[1,28,32] When comparing different catalysts (Figure 3D), altering the anion of the tetrabutylammonium cation from bromide to chloride, the conversion drops from 68 to 52%, which is supported by the literature.^[16,83] This result is ascribed to the bulkiness of the tetrahedral ammonium ion, which forces the halide anion away from the cation. This reduced electrostatic interaction renders the halide anion (i.e., Cl⁻ or Br⁻) more nucleophilic.^[84] Since the bromide anion is bulkier than the chloride anion, when pushed away from the cation, the bromide anion reacts more quickly as a nucleophile in the attack of the epoxide ring. The bromide anion is also a better-leaving group, which facilitates the ring-closing step and formation of the cyclic carbonate. Comparing catalysts TBACl and VBACl, the former renders a higher conversion than the latter (conversions of 52% and 41%, respectively). This result is believed to be because VBACl tends to polymerize with the increase of temperature, thus creating a competition between the polymerization reaction and the conversion reaction and due to the degradation that the co-catalyst suffered over time after having been synthesized in the

laboratory. Catalyst PVBACl increased the viscosity during the reaction, which encompassed the porous carbon. The low conversion of 14% is ascribed to the viscosity of the paste, which limited the migration of the reactant to the catalytic sites and, consequently, led to a lower conversion due to poor diffusion.^[77]

The study of the evolution of the conversion over time (Figure 3E) found that the maximum conversion (≈100%) was reached when the reaction lasted 24 h, both with and without the CHI-ImCl. For the intermediary reaction times tested (3 and 8 h), the reaction containing the porous carbon consistently yielded greater conversion than the reaction without it, which confirms the important role of the carbonaceous support during the reaction. Furthermore, the reaction with the CHI-ImCl present reaches a high conversion (>95%) in, at least, 8 h, which is lower than those found in the literature.^[28,32]

Figure 3F summarizes the results of the cycloaddition reaction of CO₂ to SO, using all the carbonaceous materials prepared, under the same conditions. The complete list of experiments and controls can be seen in Table S2 (Supporting Information). When comparing the type of biomass used to produce the porous carbon, the samples produced with primary sludge (PriS-0) and knots (Kno-0) exhibited the lowest conversions of 47% and 50%, respectively, while the sample produced from biological sludge (BioS-0) had the highest conversion of 75%, which surpassed that of the sample prepared with chitosan (CHI-0). This result might be explained by the presence of carbonate ions in sample BioS-0 detected with Raman spectroscopy, and by the presence of heteroatoms such as silicon, magnesium, and phosphorus. It has been reported that alkali metal carbonates can be used as activating agents for inducing microporosity and increasing surface area,^[85] which means that the carbonates present in the biological sludge could have kickstarted a chemical activation, which impacted the conversion positively. Also, the heteroatoms in the biological sludge can contribute to additional active sites, working as Lewis acids that can activate the epoxide substrate and/or as Lewis acid or bases that are capable of CO₂ activation.^[86] Furthermore, when the IL additive Im[Cl] was used with the biological sludge to produce sample BioS-ImCl, there was an improvement of the conversion from 75% to 81%, the highest conversion obtained in this study, in comparison to the other porous carbon. This improvement can be attributed to the increased nitrogen content, as shown through elemental analysis (Entry 7 and 8 of Table 1), and the consequent increase in active sites from the incorporation of the imidazolium-based IL. This result reinforces the possibility of using waste materials, such as the biological sludge supplied by The Navigator Company, for carbonaceous support production.

There is an overall improvement in the conversion when additives are also used as carbon precursors, both in the case of the porous carbons produced from biological sludge or chitosan (Table S2, Supporting Information). The use of porous supports from different carbonization batches does not affect the outcome of the catalytic conversion, as the conversion rates remain consistent across batches, indicating the reliability and robustness of the experimental procedure.

The reaction with the CHI-ImCl in the presence of catalyst TBABr achieved the highest conversion of 80% for the samples prepared with chitosan. This result might be explained by the respective nitrogen atoms, since these favor the interactions

between the active phase and the support, and can even have direct participation in the reaction mechanism, which benefits the conversion.^[87] However, the nitrogen content of this sample was relatively low (Entry 10 of Table 1), so there is possibly a better distribution throughout the carbon's surface improving their performance as basic active sites and promoting the CO₂ conversion.

Overall, while the yield and selectivity of CO₂ cycloaddition reactions are predominantly influenced by the IL catalysts, the nature of the carbon material can also impact this yield, likely by enhancing CO₂ adsorption and/or stabilizing reaction intermediates. The major difference between biomass-derived sources, such as chitosan-derived materials and the paper mill waste sludges and knots, lies in their elemental composition, which in turn affects the morphology and structure of the carbonized materials. Consequently, the composition of the carbonaceous materials modulates the interactions between IL catalysts or intermediates and the carbon, as well as between CO₂ and the carbon. Focusing on the most effective materials, CHI and BioS, while CHI-derived materials exhibit mainly carbon and nitrogen content, the predominant presence of oxygen, carbon, and calcium elements in BioS is noteworthy. A comparative analysis of catalysis outcomes using these carbonaceous supports reveals that the heterogeneous composition of BioS engenders a synergistic effect, facilitating CO₂ adsorption via acid-base interactions or anchoring effects, thereby enhancing reaction yield.

To assess the stability and reusability of the BioS-ImCl as catalyst support, it was submitted to 5 recycle runs, after each of which the reaction product was analyzed through ¹H NMR. As displayed in Figure 3G, after 5 recycle runs, there is no alteration in the selectivity, which is maintained constant at >99%, and no decrease was detected in the conversion to SC, demonstrating that the BioS-ImCl impregnated with TBABr hybrid catalyst maintained its catalytic activity after use.

4. Conclusion

The conversion of CO₂ into added-value products is imperative to provide a solution whenever no non-CO₂-emitting alternatives are at hand. Given the low reactivity of CO₂, catalysts are needed to enable these reactions, however, the production of such species should avoid unnecessary CO₂ emissions. The carbonization of waste biomass materials into porous carbons delivers at the same time a recycling approach and porous carbon production. The present work evaluated the behavior of paper mill residues and chitosan as hybrid catalysts precursors, which were later tested in the CO₂ cycloaddition to styrene oxide. ILs were used concomitantly with the biomass residues as additives during the hydrothermal carbonization before the carbonization in nitrogen flow. Carbonization yields between 22% and 41% were obtained, with an increase in overall carbon content and a decrease in nitrogen and hydrogen content. The introduction of ILs in the hydrothermal carbonization increased the average nitrogen content in the order: imidazolium < pyridinium < pyrrolidinium. The porous carbons have essentially macroporosity and some mesoporosity. Their evaluation as catalyst supports in the cycloaddition reaction of CO₂ to styrene oxide obtained a maximum conversion of 98% and selectivity >99% using BioS-ImCl/TBABr as hybrid catalyst, at 100 °C and 5 bar CO₂ pressure, with 3.5 mol% of TBABr. The recyclability of this catalyst support was demon-

strated along 5 consecutive reaction cycles. The waste biomass residues from paper mill biological sludges proved to be excellent hybrid catalysts precursors via carbonization in the presence of ImCl to obtain an effective CO₂ conversion, closing the loop on both wastes: CO₂ and biomass residues.

Supporting Information

Supporting Information is available from the Wiley Online Library or from the author.

Acknowledgements

M.Z. thanks the funding received from the European Union's Horizon 2020 research and innovation program under the Marie Skłodowska-Curie Individual Fellowships (GA no. 101026335). M.C.C. thanks FCT for the researcher contract 2021.03255.CEECIND. The authors acknowledge the support of FCT- Fundação para a Ciência e a Tecnologia, I.P., in the scope of the projects PTDC/QUI-QFI/31508/2017, and LA/P/0037/2020, UIDP/50025/2020 and UIDB/50025/2020 of the Associate Laboratory Institute of Nanostructures, Nanomodelling and Nanofabrication-i3N, UIDB/00729/2020 and UIDP/00729/2020 of VICARTE, and also PT-NMR/ROTEIRO/0031/2013 and PINFRA/22161/2016.

Conflict of Interest

The authors declare no conflict of interest.

Data Availability Statement

The data that support the findings of this study are available from the corresponding author upon reasonable request.

Keywords

biomass, carbonization, CO₂ cycloaddition, ionic liquids, paper mill sludge

Received: December 20, 2023

Revised: April 3, 2024

Published online:

- [1] L. Muniandy, F. Adam, N. R. A. Rahman, E. P. Ng, *Inorg. Chem. Commun.* **2019**, 104, 1.
- [2] M. Buaki-Sogó, A. Vivian, L. A. Bivona, H. García, M. Gruttadauria, C. Aprile, *Catal. Sci. Technol.* **2016**, 6, 8418.
- [3] Z. Akbari, M. Ghiaci, *Ind. Eng. Chem. Res.* **2017**, 56, 9045.
- [4] J. Sun, J. Wang, W. Cheng, J. Zhang, X. Li, S. Zhang, Y. She, *Green Chem.* **2012**, 14, 654.
- [5] R. Wang, J. Wan, H. Guo, B. Tian, S. Li, J. Li, S. Liu, T. D. James, Z. Chen, *Carbon N Y* **2023**, 211,.
- [6] C. Claver, M. Bin Yeamin, M. Reguero, A. M. Masdeu-Bultó, *Green Chem.* **2020**, 22, 7665.
- [7] N. A. M. Razali, K. T. Lee, S. Bhatia, A. R. Mohamed, *Renewable Sustainable Energy Rev.* **2012**, 16, 4951.
- [8] Y. He, D. Jiang, X. Li, J. Ding, H. Li, H. Wan, G. Guan, *J. CO₂ Util.* **2021**, 44, 101427.

- [9] J. N. Appaturi, R. J. Ramalingam, M. K. Gnanamani, G. Periyasami, P. Arunachalam, R. Adnan, F. Adam, M. D. Wasimiah, H. A. Al-Lohedan, *Catalysts* **2020**, *11*, 4.
- [10] P. Mao, W. Dai, W. Yang, S. Luo, Y. Zhang, J. Mao, X. Luo, J. Zou, *J. CO₂ Util.* **2018**, *28*, 96.
- [11] W. J. Peppel, *Ind. Eng. Chem.* **1958**, *50*, 767.
- [12] S. K. Shukla, S. G. Khokarale, T. Q. Bui, J.-P. T. Mikkola, *Front Mater* **2019**, *6*, 1.
- [13] C. Calabrese, F. Giacalone, C. Aprile, *Catalysts* **2019**, *9*, 325.
- [14] B. Cornils, W. A. Herrmann, J. H. Xu, H. W. Zanthoff, *Catalysis from A to Z: A Concise Encyclopedia*, 5th Edition, **2019**.
- [15] M. Cozzolino, K. Press, M. Mazzeo, M. Lamberti, *ChemCatChem* **2016**, *8*, 455.
- [16] A. Lopes do Rosário Ventura, *Utilization of Ionic Liquids as Solvents and Co-Catalysts in the Production of Cyclic Carbonates from CO₂*, Universidade Nova de Lisboa, Lisbon, Portugal **2017**.
- [17] Z.-Z. Yang, L.-N. He, Y.-N. Zhao, B. Li, B. Yu, *Energy Environ. Sci.* **2011**, *4*, 3971.
- [18] L. Guo, K. J. Lamb, M. North, *Green Chem.* **2021**, *23*, 77.
- [19] M. F. Rojas, F. L. Bernard, A. Aquino, J. Borges, F. D. Vecchia, S. Menezes, R. Ligabue, S. Einloft, *J. Mol. Catal. A Chem* **2014**, *392*, 83.
- [20] Y. Wang, J. Nie, C. Lu, F. Wang, C. Ma, Z. Chen, G. Yang, *Microporous Mesoporous Mater.* **2020**, *292*, 109751.
- [21] J. Kim, S. N. Kim, H. G. Jang, G. Seo, W. S. Ahn, *Appl Catal A Gen* **2013**, *453*, 175.
- [22] Y. Li, B. Zou, C. Hu, M. Cao, *Carbon N Y* **2016**, *99*, 79.
- [23] W. Cheng, X. Chen, J. Sun, J. Wang, S. Zhang, *Catal. Today* **2013**, *200*, 117.
- [24] A. I. Adeleye, D. Patel, D. Niyogi, B. Saha, *Ind. Eng. Chem. Res.* **2014**, *53*, 18647.
- [25] N. M. Julkapli, S. Bagheri, *Int. J. Hydrogen Energy* **2015**, *40*, 948.
- [26] M. C. Román-Martínez, C. Salinas-Martínez de Lecea, in *New and Future Developments in Catalysis: Hybrid Materials, Composites, and Organocatalysts*, Elsevier, Amsterdam, Netherlands **2013**, pp. 55–78.
- [27] T. Chen, Y. Peng, M. Qiu, C. Yi, Z. Xu, *Coord. Chem. Rev.* **2023**, *489*.
- [28] W. Kong, J. Liu, *RSC Adv.* **2019**, *9*, 4925.
- [29] X. Ma, B. Zou, M. Cao, S.-L. Chen, C. Hu, *J. Mater. Chem. A* **2014**, *2*, 18360.
- [30] X. Shao, Y. Zhang, X. Miao, W. Wang, Z. Liu, Q. Liu, T. Zhang, J. Ji, X. Ji, *Sustainable Energy Fuels* **2021**, *5*, 4701.
- [31] A. Samikannu, L. J. Konwar, P. Mäki-Arvela, J. P. Mikkola, *Appl. Catal. B* **2019**, *241*, 41.
- [32] R. A. Molla, A. Iqbal, K. Ghosh, M. Islam, *ChemistrySelect* **2016**, *1*, 3100.
- [33] J. A. O. Chagas, G. O. Crispim, B. P. Pinto, R. A. S. San Gil, C. J. A. Mota, *ACS Omega* **2020**, *5*, 29520.
- [34] Q. Wu, M. Gao, G. Zhang, Y. Zhang, S. Liu, C. Xie, H. Yu, Y. Liu, L. Huang, S. Yu, *Nanotechnology* **2019**, *30*, 185702.
- [35] Z. Liu, Z. Zhang, Z. Jia, L. Zhao, T. Zhang, W. Xing, S. Komarneni, F. Subhan, Z. Yan, *Chem. Eng. J.* **2018**, *337*, 290.
- [36] Y. J. Heo, S. J. Park, *Energy* **2015**, *91*, 142.
- [37] D. Li, T. Ma, R. Zhang, Y. Tian, Y. Qiao, *Fuel* **2015**, *139*, 68.
- [38] J. N. Appaturi, F. Adam, *Appl. Catal. B* **2013**, *136–137*, 150.
- [39] F. Adam, J. N. Appaturi, E. P. Ng, *J. Mol. Catal. A Chem.* **2014**, *386*, 42.
- [40] R. J. Ramalingam, J. N. Appaturi, T. Pulingam, N. Ibrahim S, H. A. Al-Lohedan, *Mater. Chem. Phys.* **2019**, *233*, 79.
- [41] B. Adeniran, R. Mokaya, *Chem. Mater.* **2016**, *28*, 994.
- [42] L. Cibien, M. Parot, P. N. Fotsing, P. Gaveau, E. D. Woumfo, J. Vieillard, A. Napoli, N. Brun, *Green Chem.* **2020**, *22*, 5423.
- [43] A. Zielińska, P. Oleszczuk, B. Charmas, J. Skubiszewska-Zięba, S. Pasiieczna-Patkowska, *J. Anal. Appl. Pyrolysis* **2015**, *112*, 201.
- [44] P. Devi, A. K. Saroha, *Bioresour. Technol.* **2015**, *192*, 312.
- [45] V. M. Monsalvo, A. F. Mohedano, J. J. Rodriguez, *Chem. Eng. Res. Des.* **2012**, *90*, 1807.
- [46] G. Gascó, C. G. Blanco, F. Guerrero, A. M. M. Lázaro, *J. Anal. Appl. Pyrolysis* **2005**, *74*, 413.
- [47] A. Bagreev, T. J. Bandoz, D. C. Locke, *Carbon N Y* **2001**, *39*, 1971.
- [48] L. Guo, R. Zhang, Y. Xiong, D. Chang, H. Zhao, W. Zhang, W. Zheng, J. Chen, X. Wu, *Molecules* **2020**, *25*, 3627.
- [49] S. Sadjadi, *Emerging Carbon Materials for Catalysis*, Elsevier, Amsterdam, Netherlands **2021**.
- [50] P. Walden, *Bulletin de l'Académie Impériale des Sciences de St.-Petersbourg* **1914**, *8*, 405.
- [51] M. C. Corvo, J. Sardinha, T. Casimiro, G. Marin, M. Seferin, S. Einloft, S. C. Menezes, J. Dupont, E. J. Cabrita, *ChemSusChem* **2015**, *8*, 1935.
- [52] M. Zanatta, N. M. Simon, J. Dupont, *ChemSusChem* **2020**, *13*, 3101.
- [53] W. Silva, M. Zanatta, A. S. Ferreira, M. C. Corvo, E. J. Cabrita, *Int. J. Mol. Sci.* **2020**, *21*, 7745.
- [54] Q. Wu, G. Zhang, M. Gao, L. Huang, L. Li, S. Liu, C. Xie, Y. Zhang, S. Yu, *J. Alloys Compd.* **2019**, *786*, 826.
- [55] Z.-L. Xie, R. J. White, J. Weber, A. Taubert, M. M. Titirici, *J. Mater. Chem.* **2011**, *21*, 7434.
- [56] S. M. Mahurin, P. F. Fulvio, P. C. Hillesheim, K. M. Nelson, G. M. Veith, S. Dai, *ChemSusChem* **2014**, *7*, 3284.
- [57] N. Fechner, T. P. Fellingner, M. Antonietti, *Adv. Mater.* **2013**, *25*, 75.
- [58] J. Gong, J. Zhang, H. Lin, J. Yuan, *Appl. Mater. Today* **2018**, *12*, 168.
- [59] X. Wang, S. Dai, *Angew. Chem., Int. Ed.* **2010**, *49*, 6664.
- [60] M. Stanton Ribeiro, M. Zanatta, M. C. Corvo, *Fuel* **2022**, *327*, 215195.
- [61] J. Yuan, C. Giordano, M. Antonietti, *Chem. Mater.* **2010**, *22*, 5003.
- [62] A. Haile, G. G. Gelebo, T. Tesfaye, W. Mengie, M. A. Mebrate, A. Abuhay, D. Y. Limeneh, *Bioresour. Bioprocess* **2021**, *8*, 35.
- [63] R. Peretz, E. Sterenzon, Y. Gerchman, V. Kumar Vadivel, T. Luxbacher, H. Mamane, *Carbohydr. Polym.* **2019**, *216*, 343.
- [64] E. I. N. C. Assis, E. M. N. Chirwa, *Can. J. Chem. Eng.* **2023**, *101*, 1123.
- [65] M. Tawalbeh, A. S. Rajangam, T. Salameh, A. Al-Othman, M. Alkasrawi, *Int. J. Hydrogen Energy* **2021**, *46*, 4761.
- [66] Q. Wu, M. Gao, G. Zhang, Y. Zhang, S. Liu, C. Xie, H. Yu, Y. Liu, L. Huang, S. Yu, *Nanotechnology* **2019**, *30*, 185702.
- [67] R. Sun, K. M. Meek, H. C. Ho, Y. A. Elabd, *Polym. Int.* **2019**, *68*, 1599.
- [68] M. N. Ettish, G. S. El-Sayyad, M. A. Elsayed, O. Abuzalat, *Environm. Chall.* **2021**, *5*, 100208.
- [69] R. Sun, K. M. Meek, H. C. Ho, Y. A. Elabd, *Polym. Int.* **2019**, *68*, 1599.
- [70] P. Hu, D. Meng, G. Ren, R. Yan, X. Peng, *Appl. Mater. Today* **2016**, *5*, 1.
- [71] L. Xiaojiang, H. Jun-ichiro, L. Chun-Zhu, *Fuel* **2006**, *85*, 1700.
- [72] A. K. Mondal, K. Kretschmer, Y. Zhao, H. Liu, C. Wang, B. Sun, G. Wang, *Chem.–Eur. J.* **2017**, *23*, 3683.
- [73] J. Urmos, S. K. Sharma, F. T. Mackenzie, *Am. Mineral.* **1991**, *76*, 641.
- [74] G. Jaria, C. P. Silva, C. I. A. Ferreira, M. Otero, V. Calisto, *J. Environm. Manag.* **2017**, *188*, 203.
- [75] M. Thommes, K. Kaneko, A. V. Neimark, J. P. Olivier, F. Rodriguez-Reinoso, J. Rouquerol, K. S. W. Sing, *Pure Appl. Chem.* **2015**, *87*, 1051.
- [76] P. Zhang, J. Yuan, T.-P. Fellingner, M. Antonietti, H. Li, Y. Wang, *Angew. Chem., Int. Ed.* **2013**, *52*, 6028.
- [77] K. Kiatkittipong, M. A. A. Mohamad Shukri, W. Kiatkittipong, J. W. Lim, P. L. Show, M. K. Lam, S. Assabumrungrat, *Processes* **2020**, *8*, 548.
- [78] P. P. Pescarmona, M. Taherimehr, *Catal. Sci. Technol.* **2012**, *2*, 2169.
- [79] F. Zhang, Y. Wang, X. Zhang, X. Zhang, H. Liu, B. Han, *Green Chem. Eng.* **2020**, *1*, 82.
- [80] B. Han, T. Wu, *Encyclopedia of Sustainability Science and Technology*, Springer, Berlin, Germany **2019**.

- [81] J. Sun, W. Cheng, W. Fan, Y. Wang, Z. Meng, S. Zhang, *Catal. Today* **2009**, *148*, 361.
- [82] R. Jamil, L. C. Tomé, D. Mecerreyes, D. S. Silvester, *Aust. J. Chem.* **2021**, *74*, 767.
- [83] X. Fu, D. Zhou, K. Wang, H. Jing, *J. CO₂ Utiliz.* **2016**, *14*, 31.
- [84] V. Caló, A. Nacci, A. Monopoli, A. Fanizzi, *Org. Lett.* **2002**, *4*, 2561.
- [85] B. Viswanathan, P. Neel, T. Varadarajan, *Methods of Activation and Specific Applications of Carbon Materials*, Research Gate, Berlin, Germany **2009**.
- [86] T. Yan, H. Liu, Z. X. Zeng, W. G. Pan, *J. CO₂ Utiliz.* **2023**, *68*, 102355.
- [87] G. R. Bolzan, G. Abarca, W. D. G. Gonçalves, C. F. Matos, M. J. L. Santos, J. Dupont, *Chem.–Euro. J.* **2018**, *24*, 1365.